Characterization of 0.18µm CMOS Ring Oscillator at Liquid Helium Temperature

Chao Luo, Tengteng Lu, Zhen Li, Jie He, Guoping Guo Key Laboratory of Quantum Information University of Science and Technology of China Hefei, China gpguo@ ustc.edu.cn

Chao Luo, Tengteng Lu, Zhen Li
Department of physics
University of Science and Technology of China
Hefei, China
lc0121@mail.ustc.edu.cn

Abstract—This paper presents low power dissipation, low phase noise ring oscillators (ROs) based on Semiconductor Manufacturing International Corporation (SMIC) 0.18µm CMOS technology at liquid helium temperature (LHT). First, the characterization and modelling of CMOS at LHT are presented. The temperature-dependent device parameters are revised and the model then shows good agreement with the measurement results. The ring oscillator is then designed with energy efficiency optimization by application of forward body biasing (FBB). FBB is proposed to compensate for the threshold voltage (V_{TH}) shift to preserve the benefits of the enhancement of the carrier mobility at 4.2K. The delay per stage (τ_p) , the static current (I_{STAT}), the dynamic current (I_{DYN}), the power dissipation (P) and the phase noise (L(foff)) are analyzed at both 298 K and 4.2 K, with and without FBB. The performance of the designed RO in terms of speed ($\tau_p=179$ ps), static current (23.55nA/stage), power dissipation (2.13µW) and phase noise (-177.57dBc/Hz@1MHz) can be achieved at 4.2K with the supply voltage (V_{DD}) reduced to 0.9V.

Keywords: cryo-CMOS; ring oscillator; power efficiency optimization

I. INTRODUCTION

With the development of quantum computing, the wiring requirements between the cryogenic quantum processor and the room temperature (RT) read-out controller can be both expensive and unreliable [1]. As an alternative, a cryogenic electronic interface that consists of control, interaction and read-out stages has been proposed. Cryogenic CMOS technology (cryo-CMOS) offers a scalable solution for quantum device interface fabrication [2]. The characteristics of metal-oxide semiconductor field-effect transistors

(MOSFETs) change because of freeze-out effect, thus stimulating a requirement for a revised SPICE model of these devices and circuit designs to be developed for use at cryogenic temperatures.

Therefore, this paper describes a study of the characterization of SMIC 0.18µm CMOS ROs down to 4.2K. Characterization and modelling of MOSFETs are performed. The RO performance in terms of delay per stage (τ_p) , static current (I_{STAT}), dynamic current (I_{DYN}), power dissipation (P) and phase noise (L(f_{off})) is studied at both 298K and 4.2K for V_{DD} ranging from 0.9V to 1.8V. Cryogenic effects on the RO performance are studied with and without FBB. The ROs have lower phase noise at 4.2K than at room temperature, while the phase noise would slightly increase as the FBB is applied. It is demonstrated that V_{DD} can be reduced down to 0.9V by appropriate application of body biasing while maintaining an ultralow total power dissipation. In addition, the application of FBB takes advantage of both equivalent speed and lower power dissipation at the low-V_{DD} case, compared to the case of high-V_{DD}.

TABLE I. SUMMARY OF CHARACTERIZED DEVICES

Device Size	Thin-oxide (3.87nm) NMOS/PMOS			
	W(µm)	L(µm)		
	0.22	0.18		
SMIC 0.18 μm	10	10		
	10	0.6		
	10	0.2		
	10	0.18		
	10	0.16		
technology				

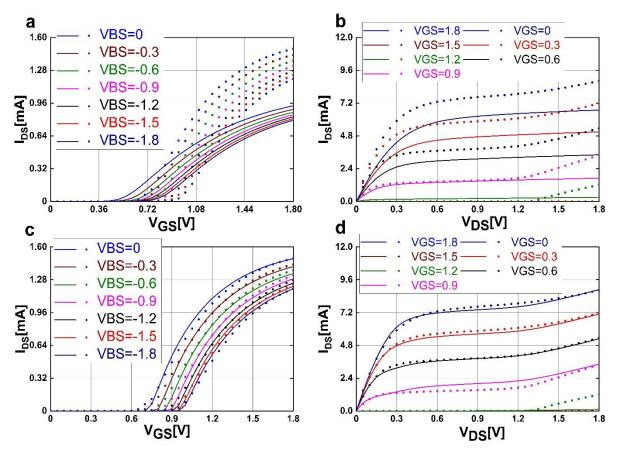


Figure 1 Device measurement and modelling, device size $W/L=10\mu m/0.16\mu m$. (a,b) $I_{DS}-V_{GS}$ curves (a) and $I_{DS}-V_{DS}$ (b) at RT (solid lines) and LHT (dashed lines); (c,d) Modelling (solid lines) and measurements (dashed lines) of at LHT

II. CMOS DEVICE MODELLING

The measurements of the CMOS transistors were performed using thin-oxide (3.87 nm) SMIC 0.18µm technology and for a wide range of feature sizes (TABEL I). All electrical measurements were performed using an Agilent B1500A semiconductor device analyzer. The cryogenic measurements were performed in the liquid helium Dewar. The most noticeable irregularity in the drain-source currentvoltage (I_{DS}-V_{DS}) characteristics (Fig.1b) is the kink that occurs in the mid- V_{DS} range at 4.2K. This phenomenon is ascribed to the self-polarization of the bulk at cryogenic temperatures [3]. In this paper, temperature-dependent parameter extraction and a sub-circuit model were applied to eliminate the deviations between the RT BSIM3 model and the measured values [4,5]. The extraction procedure was performed using BsimProPlus and model revision was performed using Matlab. As shown in Fig.1, good agreement with the measurements was achieved for devices operating at LHT. Significant optimization of the BSIM3 model thus been achieved.

III. CIRCUIT DESCRIPTION

The gate width/length of both NMOS and PMOS transistors are $0.22\mu m/0.18\mu m$. The layout of RO is shown schematically in Fig. 2a, while Fig. 2b shows a schematic of the single inverter stage composed of NMOS and PMOS transistors. The RO consists of 101 identical stages combined with an enabling two-way AND gate. The parameters and measurements protocols are listed in Table II.

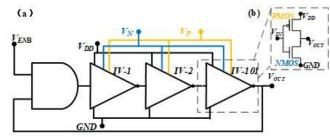


Figure 2 Schematic of 101-stages RO circuit (a) and single inverter stage (b).

The impulse sensitivity function (ISF) is introduced to describe the sensitivity of every point of the wave form to a perturbation in single-ended ring oscillators [6] and the single-

sideband phase-noise spectrum due to a white-noise current source is given by [7]

$$L\{f_{off}\} = \frac{r_{rms}^2}{8\pi^2 f_{off}^2} \cdot \frac{i_n^2/\Delta f}{q_{max}^2}$$
 (1)

where Γ_{rms} is the root mean square (RMS) value of the ISF, $i_n^2/\Delta f$ the single-sideband power spectral density of the noise current source, q_{max} given by the relation $q_{max} = C_L V_{DD}$, f_{off} the frequency offset from the carrier.

According to [6], the approximate expression for Γ_{rms} is obtained:

$$\Gamma_{rms} = \sqrt{\frac{2\pi^2}{3\eta^3}} \frac{1}{N^{1.5}} \tag{2}$$

where η is a proportionality constant, which is typically close to one and N is the number of stages of RO.

For single-ended N-stages CMOS ring oscillators, assuming that the thermal noise sources of every inverter are uncorrelated and that the waveform (hence the ISF) of all nodes are the same except for a phase-shift, the total phase noise is N times the value given by (1). Taking only these inevitable noise sources into account, the expression for phase noise is given by [6]:

$$L\{f_{off}\} \approx \frac{8}{3\eta} \cdot \frac{\kappa T}{P} \frac{V_{DD}}{V_{char}} \cdot \frac{f_0^2}{f_{off}^2}$$
 (3)

where κ is the Boltzmann constant, T the temperature, V_{DD} the operating voltage, f_0 the frequency of RO, P the total power dissipation, V_{char} the characteristic voltage of the device.

The total power dissipation *P* is approximately given by $P = 2\eta NV_{DD}q_{max}f_0 \qquad (4)$

For short-channel mode of operation, the V_{char} is defined

as

$$V_{char} = \frac{E_c L}{\gamma} \tag{5}$$

where E_c is defined as the value of electric field resulting in half the carrier velocity expected from low field mobility, L is the gate-length and γ is 2/3 for long-channel devices in saturation region and 2~3 times greater for the case of short-channel devices. Note the absence of any dependency on the number of stages in (3).

TABLE II. RO PARAMETERS, UNITS, DESCRIPTION, AND THE MEASUREMENT PROTOCOL

Parameter	Unit	Description	Measurement protocol	
f	Hz	RO frequency	$V_{ENB}=V_{DD}, V_{CC}=1$ V	
			and measure OUT.	
$ au_p$	ps	RO delay per	$=1/(f \times 2 \times N)$	
		stage		
ISTAT	pA/stage	Static current per	$V_{ENB} = V_{CC} = GND$	
		stage in non-	and measure OUT.	
		oscillating		
		state		
I_{DYN}	nA/stage	Dynamic current	$V_{ENB}=V_{DD},$	
		per stage in	V _{CC} =GND and	
		oscillating	measure OUT	
		state		
P	μW	Total Power	$=(I_{DYN}-I_{STAT}) \times V_{DD}$	
		dissipation		
$L(f_{off})$	dBc/Hz	Phase noise	Equation (3)	

IV. SIMULATION RESULTS

The static current per stage generated by leakage from the supply to ground of the 101-stages RO is shown in Table 2 for a set of V_{DD} . The static current (and thus the static power consumption) shows a significant decrease with temperature decreases. The delay per stage of CMOS inverter is given approximately by $\tau_p = C_L \times V_{DD}/I_{EFF}$, where I_{EFF} is the effective current [8] and C_L is the load capacitance, which includes the inversion capacitance, the parasitic capacitance and the wiring capacitance between the two stages. Reducing power dissipation by reducing the value of V_{DD} degrades the speed of RO, as shown in Fig. 3.

The mobility of transistor is strongly enhanced because of the reduction in carrier scattering due to lattice vibrations [4] and should thus lead to a smaller tp at LHT for a given V_{DD}. However, the RO suffers a significant reduction in operating speed, as shown in Fig.3a. This increase in the delay per stage is ascribed to the V_{TH} shift (Fig. 1a) that occurs at LHT for both NMOS and PMOS transistors. It should be noted that the load capacitance is weakly dependent on temperature and is a minor reason for the speed change of RO [8]. Body biasing was used to compensate the V_{TH} shift to preserve the benefit of higher carrier mobility. On reduction of temperature from RT to 4.2K, the delay per stage shows significant reductions by 75.68% at V_{DD} =0.9V, 66.33% at V_{DD} =1.2V, 56.04% at V_{DD} =1.5V, 48.49% at V_{DD} =1.8V. The τ_p of RO is $100.66 ps@V_{DD}=1.3V$ with FBB $(V_N/V_P=1.1V/-0.6V)$ and is 100.11ps@V_{DD}=1.5V without FBB, while the total power dissipation P=6.96µW and 9.68µW respectively. Equivalent speed is achieved by applying FBB while the power consumption is reduced. Note that the result can be optimized by adjusting the values of FBB. Application of body biasing thus results in significant τ_p gain especially at low supply voltages, but cause a slight increase in the power dissipation, as shown in Fig. 3 and Fig. 4.

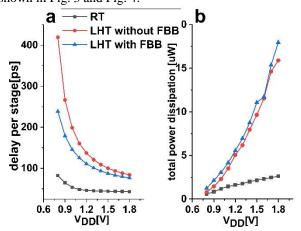


Figure 3. Comparison of ring oscillator performance at room temperature and 4.2K with and without body biasing $(V_N/V_P=1.1V/-0.6V)$: (a) comparison of energy delay per stage; (b) comparison of total power dissipation.

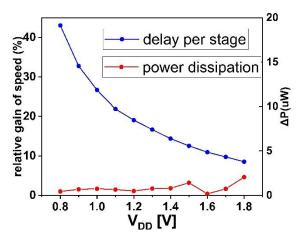


Figure 4. Power dissipation increase and relative enhancement of τ_p

Fig. 4 shows the relative enhancement of τ_p and the increased total power dissipation with and without FBB for a set of values. The RO performance in terms of τ_p , I_{DYN} , I_{STAT} , P and $L(f_{off})$ (at a frequency offset of 1MHz) as measured/calculated at 4.2K and 298K with and without FBB is summarized in Table III. The phase noise decreases approximately 25dBc/Hz at 4.2K when compared to that at RT for different VDD and increases slightly when FBB is applied.

TABLE III. COMPARISON OF RO PERFORMANCE AT 298K AND 4.2K BETWEEN THE CASES WITH AND WITHOUT FBB

		Without		I_{DYN}	$\overline{}$			[3]
T	V_D	FBB	τ_p	(nA/stage)		P	$L(f_{off})$	
(K)	D	with	(ps)		/	(µW)	(dBc/Hz)	
	(V)	FBB		/				r 4-
		V_N/V_P			I_{STAT}			[4]
		(V/V)			(fA/stage)			
	0.9		64.80	9.23	2907	0.84	-154.65	
298	1.2		46.14	13.31	40594	1.61	-153.17	[5]
	1.5		44.00	14.29	63208	2.15	-152.97	
	1.8		13.16	14.46	77089	2.61	-152.88	
	0.9		266.44	16.04	0.10	1.46	-179.30	[6]
		1.1/-0.6	179.17	23.55	0.16	2.14	-177.57	۲.,
	1.2		137.06	41.87	0.13	5.07	-176.41	[7
4.2		1.1/-0.6	110.92	45.94	0.19	5.57	-175.49	Ľ,
	1.5		100.11	63.87	0.17	9.68	-175.05	
		1.1/-0.6	87.56	73.28	0.22	11.10	-174.46	
	1.8		83.79	87.66	0.20	15.94	-174.27	[8]
		1.1/-0.6	76.66	99.02	0.26	18.00	-173.89	

V. CONCLUSION

This paper describes the electrical characterization of SMIC 0.18µm CMOS ROs at temperatures down to 4.2K. It

is demonstrated that by appropriate application of the FBB, benefit in terms of both speed and power dissipation can be derived at low supply voltage of VDD=0.9V. The speed of the designed RO is significantly optimised with a small increase in power consumption. Very small power dissipation of 2.13 μ W with τp =179 ps and phase noise =-177.57 dBc/Hz@1MHz for VDD=0.9V are achieved at 4.2K. The results indicate the applicability of body biasing to the design of power-efficient peripheral circuits for large scale quantum computing.

ACKNOWLEDGMENT

The authors would like to thank SMIC for device fabrication and software support. This work was supported by the National Key Research and Development Program of China, China (Grant No.2016YFA0301700), the National Natural Science Foundation of China, China (Grant No.11625419), the Anhui initiative in Quantum information Technologies, China (Grants No.AHY080000). This work was partially carried out at the USTC Centre for Micro- and Nanoscale Research and Fabrication.

REFERENCES

- [1] E. Charbon and F. Sebastiano, "Cryo-CMOS for quantum computing," 978-7-5090-3902-9/ 16/\$31.00, IEEE; 2016.J. Clerk Maxwell, A Treatise on Electricity and Magnetism, 3rd ed., vol. 2. Oxford: Clarendon, 1892, pp.68–73.
- [2] B. Patra and E. Charbon, "Cryo-CMOS circuits and systems for quantum computing applications," IEEE J. Solid-State Circuits 2018;53(1).
 - G. Ghibaudo and F. Balestra, "Low temperature characterization of silicon CMOS devices," Proc.20th.Conf. Microelectronics. 1995. p. 613–22.
 - Z. Li, C. Luo, and et al, "Modelling and Kink Correction of 0.18μm Bulk CMOS at Liquid Helium Temperature," Electronics Letters, (submitted).
 - C. Luo, Z. Li, and et al, "MOSFET characterization and modelling at cryogenic temperatures," Cryogenics, 2019, 98:12-17. https://doi.org/10.1016/j.cryogenics.2018.12.009.
 - A. Hajimiri, S. Limotyrakis, "Jitter and Phase Noise in Oscillators," IEEE J. Solid-State Circuits, VOL.34, NO.6, JUNE 1999.
 - A. Hajimiri, T. H. Lee, "A general theory of phase noise in electrical oscillators," IEEE J. Solid-State Circuits, VOL.33, pp. 179-194, Feb.1998.
 - H. Bohuslavskyi and et al, "Cryonice Characterization of 28-nm FD-SOI Ring oscillators With Energy Efficiency Optimization," IEEE Transactions on Electron Devices, VOL.65, NO.9, September 2018.